行政院國家科學委員會補助專題研究計畫 ■ 成 果 報 告 □期中進度報告

奈米解析度記錄媒體及其他應用之包覆合金碳奈米結構陣列，

其製造、機械/熱性質及製程特徵之研究子計畫一(3/3)--

包覆磁性合金碳奈米結構陣列在奈米解析度垂直記錄媒體之應用

計畫類別： □個別型計畫　　■整合型計畫
計畫編號：NSC94－2120－M－009－003－
執行期間：94 年 8 月 1 日至 95 年 7 月 31 日

計畫主持人：郭正次 博士
共同主持人：潘扶民 博士、吳宗信 博士
計畫參與人員： 林兆君、王威翔、陳柏林、曾文綏、莊必愷、林貞君、鄧伊茹、王立群、駱安亞、汪俊翰、洪蔡豪、黃崇獻、沈煌凱

成果報告類型(依經費核定清單規定繳交)：□精簡報告　■完整報告

本成果報告包括以下應繳交之附件：
□赴國外出差或研習心得報告一份
□赴大陸地區出差或研習心得報告一份
■出席國際學術會議心得報告及發表之論文各一份
□國際合作研究計畫國外研究報告書一份

處理方式：除產學合作研究計畫、提升產業技術及人才培育研究計畫、列管計畫及下列情形者外，得立即公開查詢
□涉及專利或其他智慧財產權，□一年□二年後可公開查詢

執行單位：國立交通大學材料工程系

中　華　民　國　96　年　6　月　22　日

行政院國家科學委員會專題研究計劃成果報告

奈米解析度記錄媒體及其他應用之包覆合金碳奈米結構陣列，

其製造、機械/熱性質及製程特徵之研究子計畫一(3/3)--

包覆磁性合金碳奈米結構陣列在奈米解析度垂直記錄媒體之應用

計劃編號：NSC94-2120-M-009-003
執行期限：94 年 8 月 1 日至 95 年 7 月 31 日
主持人：郭正次　國立交通大學材料科學與工程系

Abstract

To examine effects of catalyst precursors, pretreatment methods and substrate recycling on the single-walled carbon nanotubes (SWNTs) formations, the processes were developed to synthesize various carbon nanostructures on Si wafer by the microwave plasma chemical vapor deposition (MPCVD) with CH_4 and H_2 as source gases, with $CoCrPtO_x$ and $CoCrO_x$ as catalyst precursors. The processes include; First, the buffer layer (AlON) and then catalyst precursors or catalysts (Co) were deposited on Si wafer by sputtering. The coated substrates were followed by H-plasma (in MPCVD system) or scanning local laser heating (in air by DVD dynamic tester) pretreatments to produce the well-distributed catalyst nanoparticles before nanostructures deposition by MPCVD method. The microstructures at each processing step and the as-deposited nanostructures and their properties were characterized by FE-SEM, TEM, HRTEM, Raman spectroscopy, XPS, TGA and I-V measurements. From the experimental results, the following conclusions can be drawn.

The results indicate that the well-aligned and base-growth SWNTs can be synthesized by using $CoCrPtO_x$ as catalyst precursor under H-plasma pretreatment. The as-deposited SWNTs are about ~ 2.6 nm in diameter and 40 um in length. The Raman spectra display the I_G/I_D ratio of the synthesized SWNTs can be reached to a value of ~ 43.The function of the catalyst precursor is essentially to promote miniaturization of the sizes of the catalyst nanoparticles down to about ~ 2.4 nm in diameter due to explosive chemical reactions during pretreatment process. This mechanism is based on the explosion associated with the reduction of PtO_x in the $CoCrPtO_x$ film, and Cr_2O_3 is employed to inhibit the agglomeration of nanoparticles during pretreatment and the initial stage of nanostructure deposition.

1. Introduction

SWNTs have recently been considered to be a promising candidate material for use in field emitters, nano-electronic devices (such as single electron transistors) [1,2], and others. In such applications, one of the key issues is to effectively manipulate the nanostructures at lower deposition temperatures in order to be compatible with the IC processes. Recently, low temperature processes to synthesize the catalyst-assisted SWNTs by CVD methods have been widely studied [3-5]. However, most of these deposited SWNTs show morphologies in randomly entangled fashions [6]. The methods to grow the well-aligned SWNTs on the desired locations are not quite successful

so far.

The treatment of the catalyst to minimize the catalyst particle sizes before CNTs growth represents another technological challenge in SWNTs growth. Physical vapor deposition (PVD) is the most popular approach for depositing catalytic materials, because it is highly compatible with the IC process. The catalyst films are typically treated with H-plasma to become well-distributed nano-particles, and CNT are subsequently grown from these pre-treated catalystic nano-particles. However, the agglomeration of nano-particles is unavoidable during the heating process, which does not particularly favor the fabrication of SWNTs. One way to minimize the catalyst particle size is to use the ultra-thin catalytic film, but the agglomeration effect during H-plasma pretreatment makes it difficultly to form SWNTs [6]. Although Zhong et al. [7] recently reported using Al_2O_3/Fe/Al_2O_3 with a sandwich-like structure to fabricate vertically aligned SWNTs, in which the Al_2O_3 buffer layer can inhibit the coarsening of Fe catalyst particles, the presence of the buffer layer on the top or bottom of catalyst layer raises other problems when SWNTs are used in electrical devices, such as adhesion, electrical conductivity and impurities. Accordingly, the purpose of this work was to develop a process to fabricate the well-aligned SWNTs at low temperatures without buffer layer application. The idea is to use the catalyst precursor ($CoCrPtO_x$) to promote the miniaturization of nanoparticles and to prevent the agglomeration effect during pretreatment and the initial stage of CNTs growth.

2. Experimental methods

First, the $CoCrPtO_x$ films (1, 2, 3, 5, 10 nm) to act as catalyst precursor were deposited by physical vapor deposition (PVD) and buffer layers (10 nm) were prepared by DC reactive sputter. H-plasma pretreatment was performed in microwave plasma chemical vapor deposition (MP-CVD) system to carry out reduction of oxidized $CoCrPtO_x$ film on silicon wafer at 30 Torr 580 ^oC 10 minutes. The specimens were subsequently heated up to grow SWNTs in an CH_4/H_2 (4/50) atmospheres for 6 minutes at 24 Torr chamber pressure. The morphologies of the pretreated catalyst precursor were studied by scanning electron microscopy (SEM). The size and distribution conditions of catalyst particles after pretreatment on the silicon wafer were characterized from grinding cross-section and plane view samples by transition electron microscopy (TEM). Additionally, X-ray photoelectron spectroscopy (XPS) was employed to characterize binding energy of $CoCrPtO_x$ layer at as-deposited and after H-plasma pretreatment to analyze the self-assembly mechanism. The morphologies, microstructures and bonding structures of the as-grown SWNTs were investigated by SEM, TEM and Raman spectroscopy with a 632.8 nm He-Ne laser, etc.

3. Results and discussion

Figure 1 illustrates the typical SEM morphologies of the pretreated catalyst precursor on silicon wafer without application of buffer layer and with various $CoCrPtO_x$ catalyst precursor thicknesses: (a) 10 nm, (b) 5 nm, (c) 3 nm, (d) 2 nm, (e) 1 nm and (f) 1 nm, respectively, except Fig. 1(f) is the catalyst precursor morphology with 10 nm AlON as buffer layer. It indicates that the average catalyst size after pretreatment is smaller for the smaller catalyst precursor thickness. By comparing the same catalyst precursor thickness but with and without buffer layer application, the specimen with buffer layer gives rise to a smaller particle size.

It is believed that very fine, dense and uniformly distributed catalyst particles after H-plasma pre-treatment can give rise to growth of the vertically and well aligned tubes due to mutual restriction between tubes. In contrast, the scarce particle distribution may result in growth of spaghetti-like CNTs. To examine this possibility, top-view and cross-sectional HRTEM micrographs of the H-plasma pre-treated catalysts without buffer layer are shown in Figs. 2(a) and 2(b), respectively. It shows uniform distributed nano-particles with diameters ranging from 3 nm to 4 nm with an average value of 3.5 nm, which is quite close to 3.2 nm from SEM examinations in Fig. 1. Effect of buffer layer on the H-plasma pretreated catalyst formation is demonstrated in Figs. 2(b) and 2(c), where the catalyst precursor-coated substrates have the same thickness, but without and with AlON buffer layer, respectively. It appears that the particle sizes after H-plasma pretreatment for the substrate with buffer layer are ranging form 1 ~ 3 nm (average 2.4 nm) corresponding value (average 3.5 nm) in Fig. 2(b). Effect of buffer layer is essentially to minimize the nano particle aggregation during H-plasma pretreatment. This is concluded from the cross-sectional view of Figs. 2(b) and 2(c), where the nano-particles seem to be trapped in the valleys of the surface, as schematically shown in Fig. 2(d). In additional to a buffer layer in Fig. 2(c), both Figs. 2(b) and 2(c) indicate formation of SiO_2 layer (~ 4 nm) after pretreatment, which is formed in the earlier stage of the pretreatment and may act as buffer layer effect in Fig. 2(b).

Figures 3(a) to 3(f) illustrate typical FESEM morphologies of the as-grown SWNTs on silicon wafer with different catalyst precursor thickness: (a) 10 nm, (b) 5 nm (c) 3 nm, (d) 2 nm, (e) 1 nm and (f) 1 nm with buffer layer. To confirm the types of CNTs precisely, Fig. 4 shows the Raman spectrum of as-grown SWNTs film, respectively. The RBM peaks in the Raman spectrum indicate the presence of SWNTs in Figs. 3(d), (e) and (f). Therefore, we demonstrate that vertically aligned SWNTs are successfully synthesized using $CoCrPtO_x$ catalyst precursor with 2 nm and 1 nm thickness. And very high I_G/I_D ratio (43/1) is obtained by 1-nm-thick catalyst precursor with 10-nm-thick AlON buffer layer.

Figures 5(a) and 5(b) show the TEM images of as-grown SWNTs with 1-nm-thick $CoCrPtO_x$ film and 10-nm-thich AlON buffer layer. The results indicate that the nanotubes are grown as SWNTs bundles with diameters of 2 to 3 nm, which resembles the diameter of catalyst particles observed by HRTEM. Therefore, each SWCNT maybe grown from individual catalytic nano-particles and the diameter of tubes is determined by sizes of the catalysts. Hardly any MWNT are founded by TEM and a very high I_G/I_D ratio (43/1) is obtained by Raman spectrum, which indicate the purification and high quality of SWNTs is good as obtained by arc-discharge which is high temperature precess.

The tilt-view of specimen presented in Figs. 6(a) and 6(b) display SWNTs film with an ultra-high density and a tube density that considerably exceeds that reported elsewhere [7]. Figure 6(c) magnifies a portion of Fig. 6(b), to show the fabrication of bundles of aligned SWNTs. Figure 6(d) shows that vertically aligned SWNTs with a height of ~40 micrometer were successfully synthesized. Notably, the SWNTs film can be easily removed from substrate and the SWNTs film is very flexible and soft, likely the woolen blanket, as shown in Fig. 6(e). Figure 6(f) shows a fragment of Si substrate with catalyst precursor which well-aligned SWNTs are magically grown exhibits the powerful growth ability of $CoCrPtO_x$ catalyst precursor.

Vertically well-aligned SWNTs films with heights of ~50 micrometer are thus concluded to fabricate successfully under the condition. By contrast, entangled SWNTs rather than aligned tubes were found in the specimens that comprised a thicker as-deposited catalyst precursor film of over

~10 nm and MWNTs are easily observed by TEM. These results are consistent with that the catalyst precursor thickness must be control at ultra thin to enable SWNTs to be synthesized.

Figures 7(a) to (c) presents the results of the XPS of the H-plasma pretreated $CoCrPtO_x$ film formed by PVD, respectively, to study how catalyst precursor can form 2~3 nm nano-particles and prevent the agglomeration of catalysts as the buffer layer did in an earlier work [6,7]. The spectra indicate that PtO_x, CrO_x and CoO_x phases are formed simultaneously in the as-deposited film during reactive sputtering deposition by PVD. Furthermore, the PtO_x associated with a peak at 74.05 eV ($4f_{7/2}$) comprises PtO (73.8 eV) and PtO_2 (74.6 eV), while CrO_x (577.4 eV) consists of CrO_2 (576.3 eV) and CrO_3 (578.3 eV), respectively. The spectrum presented in Fig. 7(a) shows that the Pt peak is shifted by 1 eV by pretreatment, indicating that most of the PtO_x atoms are reduced to Pt atoms in the H_2 atmosphere, but a small quantity of PtO_x remains. Most interestingly, the Cr phases in Cr_2O_3 remains, suggesting that the nano-particles from catalyst precursor results mostly from the reduction of PtO_x or CoO. However, the nano-sized catalysts are driven mainly by PtO_x as will be discussed in the following paragraph.

Recently, PtO_x has been demonstrated to be an active layer for use in the next generation of optical storage media applications [8], from which, oxygen is released after prolonged laser heating to compress the adjacent layers to form pits as recording marks, which consist of oxygen bubble gas and fine Pt nano-particles. Therefore, the exploding phenomenon associated with the reduction of PtO_x (PtO/PtO_2) may cause the formation of very fine particles and such self-assembly behavior may depend on the process temperature. In this experiment, a pre-treatment temperature that is too low (below 500 ^oC) results in an incomplete reduction of an oxidized CoCrPt film. In this case, non-uniform large catalytic particles are formed, and only MWNTs can be synthesized. The oxidized CoCrPt film has a higher critical self-assembly temperature than PtO_x (~500 ^oC), which difference is determined by the difference between the compositions.

With respect to the role of Cr, Cr_2O_3 can inhibit the agglomeration of particles [9]. Hence, it is believed to play a role in suppressing the agglomeration of catalytic particles in the self-assembly process. The Co element has an essential role in the dissolubility and precipitation of carbon species in the SWNTs growth because the dissolubility of carbon in Cr_2O_3 and Pt is rather small. The earlier work demonstrates that the pure Co catalytic nano-particles can also be formed by the reduction of CoO that is prepared as a chemical complex solution. However, the large sizes distribution and low density of the particles do not support SWNTs growth. The self-assembly mechanism that involves the exploding effect associated with the reduction of $CoCrPtO_x$ film enables the size and distribution of the catalysts to be manipulated to fabricate as-grown SWCNT with the desired morphology by controlling the composition, thickness and H-plasma pre-treatment temperature of the film. The effect of the composition of CoCrPt on the self-assembly of nano-particles must be discussed in the future.

4. Conclusions

In this work, the $CoCrPtO_x$ film was successfully used as catalyst precursor to grow the well-aligned SWNTs with high tube number density by MPCVD. The main mechanism to form SWNTs is due to the fact that the PtO_x in the $CoCrPtO_x$ precursor can be decomposed during pretreatment to promote miniaturization of the Co-catalyst particle due to explosive effect of the reaction. Moreover, Cr_2O_3 in the precursor can act to separate the Co-catalyst nanoparticles from agglomeration. The process also takes the advantage of recycling the catalyst-coated substrate to

minimize the processing cost. Raman spectra indicate that the I_G/I_D ratio of these SWNTs can be reached to ~ 43, indicating a good quality.

The technique supplied a powerful method to fabricate ultra-high tube density and well-aligned SWNTs for memory applications. In theoretically, we could create a larger storage medium assisted with the ferromagnetic material of CoCrPt encapsulated SWNTs arrays by magnetic recording function. However, the magnetic catalysts were observed on the base of each tube due to its repeatable growth under scraping SWNTs several times from the substrates. Therefore, in the future works, how to synthesize tip growth magnetic materials encapsulated SWNT arrays is the most important solution in storage media applications.

References

[1] Collins, P. G., M. S. Arnold, and P. Avouris, Science, 292, (2001), 706-709, “Engineering Carbon Nanotubes and Nanotube Circuits Using Electrical Breakdown”.

[2] Bachtold, A., P. Hadley, T. Nakanishi, and C. Dekker, Science, 294, (2001), 1317-1320, “Logic Circuits with Carbon Nanotube Transistors”.

[3] Qin, L. C., D. Zhou, A. R. Krauss, and D. M. Gruen, App. Phys. Lett., 72, (1998), 3437-3439, "Growing carbon nanotubes by microwave plasma-enhanced chemical vapor deposition".

[4]Kurt, R., J. M. Bonard, A. Karimi, Carbon, 39, (2001), 1723-1730, “Morphology and field emission properties of nano-structured nitrogenated carbon films produced by plasma enhanced hot filament CVD”.

[5] Tsai, M. H., M.S. Thesis, (2001), Mat. Res. Lab., MSE, NCTU, “Deposition mechanisms and properties of large area well-aligned carbon nanotubes by catalyst-assisted ECR-CVD method”.

[6] Delzeit, L., B. Chen, A. Cassell, R. Stevens, C. Nguyen, and M. Meyyappan, Chem. Phys. Lett. 348, (2001), 368-374, Multilayered metal catalysts for controlling the density of single-walled carbon nanotube growth”.

[7] Zhong G., T. Iwasaki, K. Honda, Y. Furukawa, I. Ohdomari, and H. Kawarada, Jpn. J. Appl. Phys. 44, (2005), 1558-1561, “Low Temperature Synthesis of Extremely Dense and Vertically Aligned Single-Walled Carbon Nanotubes”.

[8] Kim J., I. Hwang, D. Yoon, I. Park, D. Shin, T. Kikukawa, T. Shima, and J. Tominaga, Appl. Phys. Lett., 83, (2003), 1701-1703, “Super- resolution by elliptical bubble formation with PtOx and AgInSbTe layers”.

[9] Shaijumon M. M., N. Bejoy, and S. Ramaprabhu, Appl. Sur. Sci., 242, 192, (2002), 192-198, “Temperature dependence of radial breathing mode Raman frequency of single-walled carbon nanotubes”.

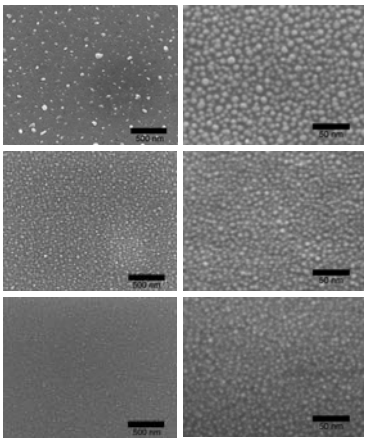

Fig. 1 Top-view SEM images of the pretreated catalyst precursor on silicon wafer without application of buffer layer and with various $CoCrPtO_x$ catalyst precursor thicknesses: (a) 10 nm, (b) 5 nm, (c) 3 nm, (d) 2 nm, (e) 1 nm and (f) 1 nm, respectively, except Fig. 1(f) is the catalyst precursor morphology with 10 nm AlON as buffer layer.

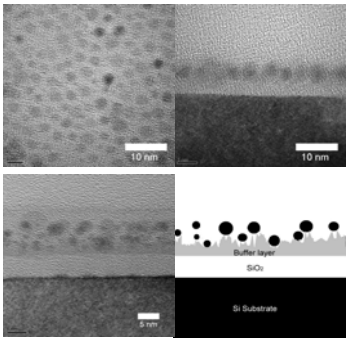

Fig. 2. HRTEM micrographs: (a) Top-view and (b) cross-section of pretreated 1 nm catalyst precursor without buffer layer. (c) Cross-section of pretreated 1 nm catalyst precursor with buffer layer. (d) Schematic diagram of Fig. 2(c).

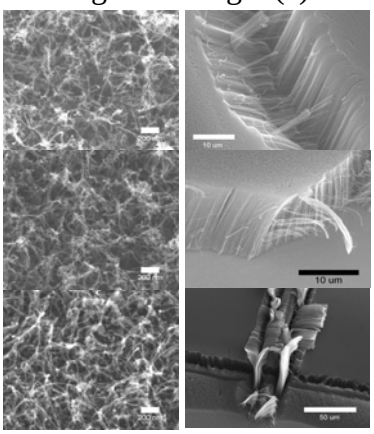

Fig. 3. SEM images of the as-grown SWNTs on silicon wafer with different catalyst precursor thickness: (a) 10 nm, (b) 5 nm (c) 3 nm, (d) 2 nm, (e) 1 nm and (f) 1 nm with buffer layer.

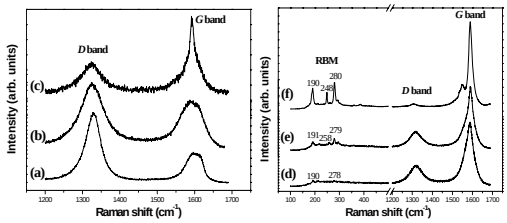

Fig. 4. Raman spectra of the as-grown SWNTs film on silicon wafer with different catalyst precursor thickness: (a) 10 nm, (b) 5 nm (c) 3 nm, (d) 2 nm and (e) 1 nm. The RBM peaks and very high intensity ratio of G-band / D-band (43:1) are found in the (f) 1-nm-thick catalyst precursor with buffer layer.

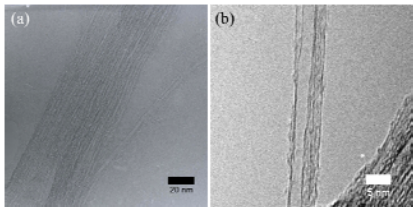

Fig. 5. HRTEM images of the typical as-grown SWNTs where the tubes are mainly bundle type and their diameters are ranged from 2~3 nm.

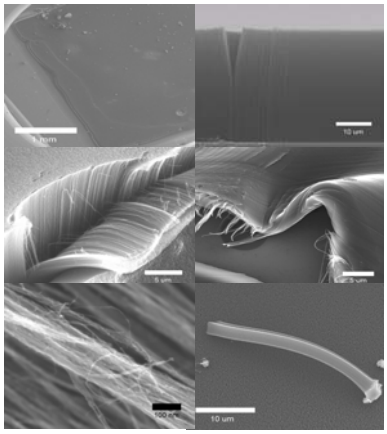

Fig. 6. Typical SEM micrographs of extremely dense and vertically aligned SWNTs film on silicon wafers: (a), (b) tilt-view, (c) is the high magnification image of (b), (d) cross-sectional view, (e) shows very flexible morphology and (f) a fragment of Si substrate, respectively.

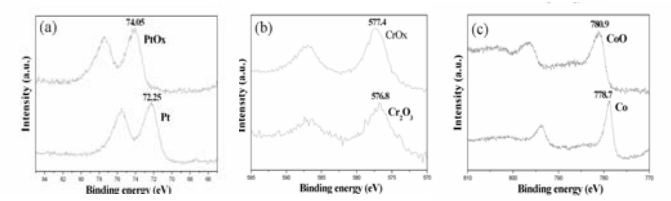

Fig. 7 XPS spectra of as-deposited $CoCrPtO_x$ film (upper curve) by PVD and after H-plasma pre-treated $CoCrPtO_x$ film (lower curve).